ОБЪЕДИНЕННЫЙ
ИНСТИТУТ
ЯДЕРНЫХ
ИССЛЕДОВАНИЙ
ДУБНА

E7 - 10229

K.-H.Kaun

THE STRUCTURE OF QUASI-MOLECULAR KX-RAY SPECTRA FROM HEAVY ION COLLISIONS

1977

E7 - 10229

K.-H.Kaun

THE STRUCTURE OF QUASI-MOLECULAR KX-RAY SPECTRA FROM HEAVY ION COLLISIONS

Proc. of the XI th Internat. School on Nuclear Physics (Heavy Ion Physics), Lecture Note, Predeal (Romania), 1976.

Каун К.Г.

E7 - 10229

Структура спектров квазимолекулярных КХ-лучей при столкновениях тяжелых ионов

Статья представляет собой лекцию, в которой автор дает обзор экспериментальных и теоретических исследований, проводившихся в последние годы для выяснения сложной структуры квазимолекулярных спектров X -лучей, возникающих при столкновениях тяжелых ионов.

Работа выполнена в Лаборатории ядерных реакций ОИЯИ.

Препринт Объединенного института ядерных исследований

Дубна 1976

Kaun K.-H.

E7 - 10229

The Structure of Quasi-Molecular KX-Ray Spectra From Heavy Ion Collisions

The paper is a review of recent experimental and theoretical investigations carried out to clarify the complex structure of quasi-molecular X-ray spectra observed in heavy ion collision at Dubna heavy ion cyclotron.

The investigation has been performed at the Laboratory of Nuclear Reactions, JINR.

Preprint of the Joint Institute for Nuclear Research

Dubna 1976

1. Introduction

The study of quasi-molecular radiation should give one a possibility of investigating two-centre systems during adiabatic collisions. This is of great importance in view of the electronic structure of heavy quasi-atoms with $Z>100$ [1,2] and for observing new processes of quantum electrodynamics in very strong electromagnetic fields [3,4]. The latter makes especially attractive experiments using very heavy ions, which involve most strongly bound states of electrons in quasi-molecules. Therefore, during the recent two years our group at Dubna have been carrying out, in the first place, experiments to study some aspects of atomic characteristics and quasi-molecular KX-rays of very heavy and symmetric collision systems such as Ni + Ni, Ge + Ge, Kr + Kr, Nb + Nb, La + La and Bi + Bi. For these heavy colliding particles, the adiabatic condition is fulfilled better than in the case of collision systems with lower Z, where the orbital velocities of electrons are rather small and the observation of quasi-molecular radiation is more difficult due to the existence of some

competing effects, which also show continuous X-ray spectra. In addition, the so far unknown properties, such as the complex structure of quasi-molecular spectra manifest themselves in experiments with heavy ions.

In this talk I would like to discuss the two-component structure of quasi-milecular spectra at energies above the energy of the characteristic atomic KX-radiation. This structure was first observed in our experiments with Ge, Nb and La ions and interpreted by our colleagues at the Institute of Nuclear Research in Rossendorf.

My talk is partially overlapping with those of Professors Greiner, Müller and Wölfli at this School. However, I hope that I shall be able to contribute to a more complete understanding of the reliability with which we can presently observe and study quasi-molecular radiation in heavy ion collisions, and outline the possibilities that can be offered by the electron states of two-centre systems for spectroscopy of superheavy quasi-atoms.

2. Experimental Methods and Background Effects

All of our experiments were carried out on an external beam from the U-300 heavy ion cyclotron of the JINR Laboratory of Nuclear Reactions with an intensity ranging from 10^{10} to 10^{12} particles/sec. Some of the symmetric collision systems investigated in our experiments, the main parameters of ion beams and the types of measurements are

given in table 1. In the quasi-molecular picture the collision is assumed to be slow enough for the electronic wavefunction in the projectile and the target atoms to adjust themselves, at each internuclear separation R, to the molecular configuration appropriate for a diatomic molecule with nuclear charges Z_1 and Z_2 and internuclear separation R. This situation occurs if the adiabaticity parameter $v_1/v_K \ll 1$, where v_1 is the projectile velocity and $v_K = (2U_K/m)^{1/2}$ is the orbital velocity of the K-shell electrons. An additional condition that makes possible the observation of quasi-molecular KX-rays is that the distance of the closest approach of the colliding nuclei is equal to or smaller than the classical Bohr radius of the K-shell in the united system. From this condition a lower limit for the projectile velocity or energy can be derived [11]. Figure 1 shows this "quasi-molecular region" of projectile energies for symmetric collision systems ($Z_1 = Z_2$) and K-shell electrons ($n = 1$) as a function of atomic number Z_1. The collision systems investigated in our experiments are placed between the two limits of this region ($1.2 \cdot 10^{-3}\ Z > v_1/C > 2 \cdot 10^{-4}\ Z$) so that we can hope to observe quasi-molecular phenomena. The principal experimental arrangement for measurements of X-ray spectra, Doppler shift and angular distribution of X-rays is very simple and is shown schematically in Figure 2. The pulsing of the cyclotron beam with 2 ms beam-on and 2 ms beam-off time offered the possibility of a simultaneous measurement of a prompt effect and delayed background by accumulating both

Table 1

Symmetric collision systems investigated in our experiments at the Dubna heavy ion cyclotron

COLLISION SYSTEM $(Z_1 + Z_2)$	ION ENERGY (MeV)	ADIABACITY PARAMETER v_1/v_K	ION INTENSITY (part./s)	MEASUREMENTS	REF.
Ni + Ni (56)	39 67	0.21 0.27	10^{12}	ATOMIC KX-RAY AND CONTINUOUS X-RAY SPECTRA	[5]
Ge + Ge (64)	54 81	0.19 0.23		DOPPLER SHIFT ANISOTROPY ANGULAR DISTR OF CONTINUOUS X - RAYS	[6]
Kr + Kr (72)	42	0.15			[7]
Nb + Nb (82)	45 67 96	0.12 0.17 0.17		INTRINSIC Ge DETECTORS $\Delta E \approx 200$ eV (at $E_x = 10$ KeV)	[8]
La + La (114)	115	0.11			[9]
Bi + Bi (166)	144 172	0.06 0.07	10^{10}		[10]

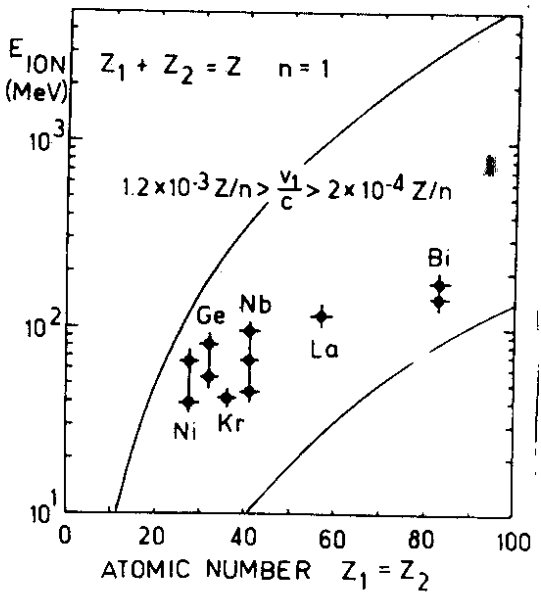

Fig.1.The "quasi-molecular region" of projectile energies for symmetric collision systems $(Z_1 = Z_2)$ and K-shell electrons (n = 1).

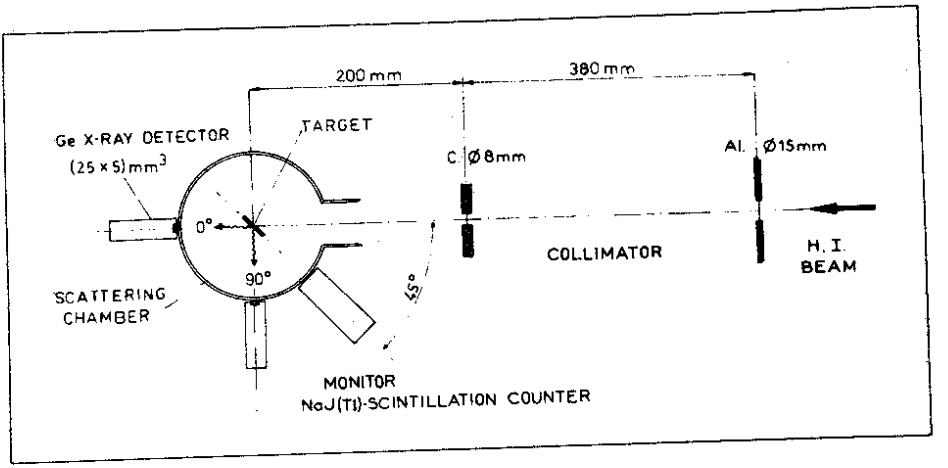

Fig. 2. The principal experimental arrangements for X-ray measurements at the heavy ion beam.

spectra in a prompt-delayed regime. Figure 3 shows a typical X-ray spectrum observed in our experiments. It was measured in the collisions of 67 MeV Nb ions with the atoms of a target made of metallic pure niobium 1 mg/cm^2 thick. The emitted X-rays were detected at 90° with respect to the ion beam axis by an intrinsic Ge detector with an energy resolution of about 200 eV at 10 KeV. The intensively excited KX-radiation of Nb atoms was strongly suppressed by using an absorber of 0.20 mm Cu. Due to a counting rate lower than 50 s^{-1}, no pile-up effects were expected in this measurement. Besides the intensive KX-lines of the Nb atoms and the absorber material, the spectrum contains a continuous intensity distribution, which ranges approximately up to the united-atom KX-energy

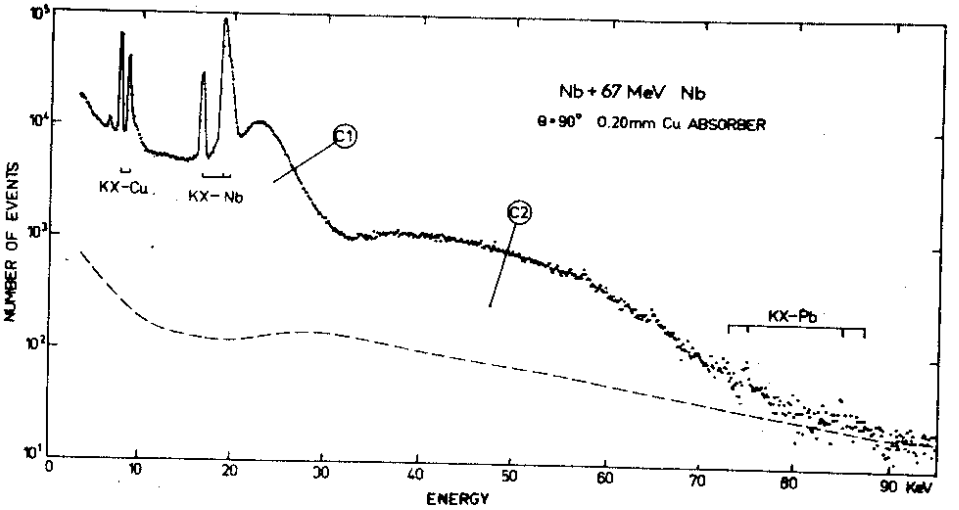

Fig. 3. The X-ray spectrum measured by bombarding the Nb target with 67 MeV Nb ions.

and is mainly formed by quasimolecular transitions. It is of interest to review the experimental evidence for this X-ray continuum situated above all the atomic characteristic KX-lines and interpreted as a quasi-molecular KX-ray spectrum (or "K - molecular orbital radiation"). Since quasi-molecular X-rays form continua one must mainly consider other continua with which quasi-molecular X-rays might be confused or which could form backgrounds under the quasi-molecular spectra. In symmetric collisions of very heavy ions the continuous background radiation can be assigned to the following processes (in addition to the normal room background):

Bremsstrahlung of secondary electrons (SEB),

Nucleus-nucleus bremsstrahlung (NNB),

Radiative electron capture (REC), and

Compton scattering of Coulomb-excited nuclear gamma-rays.

The latter type of background radiation was very small in all of our investigations. We have minimized this effect by using projectiles and targets with nuclei having high-lying excited states (Ni, Kr, Nb, Bi), or determined the shape of this small background under the X-ray continuum in experiments with Ge and La ions by using gamma-rays of similar energy from radioactive sources.

The bremsstrahlung processes (SEB and NNB) have been the subject of much theoretical and experimental study. Our group have been carrying out calculations, which allow to estimate the contributions of the electronic and nuclear bremsstrahlung to the X-ray spectra measured in our investigations. The methods of calculations are described by Gippner in Ref. /12/. The differential cross section for production of bremsstrahlung from secondary electrons by impact of heavy ions (E_1, Z_1, A_1) with target atoms (Z_2, A_2) is given by the formula

$$\frac{d^b\sigma(E_r,E_1)}{dE_r} = \int_{E_r}^{\infty} dE_\delta \frac{d\sigma_e(E_\delta,E_1)}{dE_\delta} \cdot \frac{dY(E_\delta,E_r)}{dE_r}, \qquad (1)$$

where $d\sigma_e(E_\delta,E_1)/dE_\delta$ is the differential cross section for production of secondary electrons in the energy interval $[E_\delta, E_\delta + dE_\delta]$

by an ion with the incidence energy E_1 and $dY(E_\delta,E_r)/dE_r$ is the yield of bremsstrahlung in the X-ray energy interval $[E_r,E_r+dE_r]$, induced by an δ-electron of an energy $E_\delta > E_r$. This yield is given by

$$\frac{dY(E_\delta,E_r)}{dE_r} = \int_{E_r}^{E_\delta} \frac{d\sigma_r(E_e,E_r)}{dE_r} \cdot \frac{dE_e}{m_e M_p A_2 S_2(E_e)} . \quad (2)$$

In this formula $d\sigma_r(E_e,E_r)/dE_r$ is the differential cross section for production of bremsstrahlung in the energy interval $[E_r,E_r+dE_r]$ for an electron with an energy E_e, $m_e M_p A_2 = m_2$ is the mass of a target atom (m_e = electron mass, $M_p = 1836.6$), and $S_2(E_e)$ is the stopping power in energy per mass for the electrons in the target material. Hence, the expression $dE_e/m_e M_p A_2 S_2(E_e)$ stands for the number of atoms per unit area colliding with the electron along the electron path and corresponding to the energy loss dE_e of the electron. By inserting equation (2) into (1) one obtains for the cross section of secondary electron bremsstrahlung

$$\frac{d\sigma^b(E_r,E_1)}{dE_r} = \int_{E_r}^{\infty} dE_\delta \frac{d\sigma_e(E_\delta,E_1)}{dE_\delta} \int_{E_r}^{E_\delta} \frac{d\sigma_r(E_e,E_r)}{dE_r} \cdot \frac{dE_e}{m_e M_p A_2 S_2(E_e)} . \quad (3)$$

As it is done in Folkmann's work [13] the cross section $d\sigma_e(E_\delta,E_1)/dE_\delta$ for production of secondary electrons in heavy ion impact was calculated by means of the binary encounter approximation of Garcia et al. [14] assuming the dominant interaction producing the inner-shell ionization to be a direct

energy exchange between the projectile and the atomic electron in question. In the framework of this approximation one obtains for the ionization cross section of bound s -shell electrons

$$\frac{d\sigma_e(E_\delta E_1)}{dE_\delta} = \int_0^\infty \frac{d\sigma\ (\Delta E, v_1, v_2)}{dE_\delta} f(v_2) dv_2 , \qquad (4)$$

where $d\sigma(\Delta E, v_1, v_2)/dE_\delta$ is the cross section for the exchange of an energy $\Delta E = U_s + E_\delta$ between the incident ion and the bound s-electron, whose velocity is v_2 and whose energy is $E_2 = \frac{1}{2} m_e v_2^2$. U_s is the binding energy on the s-shell. The nucleus-nucleus bremsstrahlung can be computed with good accuracy by using the theory of Alder et al. /15/. The electric dipole (E_1) component of nuclear bremsstrahlung has the highest intensity and the contributions of higher electrical multipolarities and also interference effects can be neglected in our cases of investigations. The differential cross section of this component (NNB) is

$$\frac{d\sigma^b_{E1}(E_r, E_1)}{dE_r} = 1.225 \cdot 10^{-8} Z_1^2 Z_2^2 \left[\frac{Z_1}{A_1} - \frac{Z_2}{A_2}\right]^2 \frac{A_1}{E_1 \cdot E_r} f_{E1}(\eta, \xi), \qquad (5)$$

where η is a collision parameter defined by

$$\eta = \frac{Z_1 Z_2}{2} \left[\frac{A_1}{10.008\, E_1}\right]^{1/2} \qquad (E_1 \text{ in MeV})$$

and ξ is an adiabaticity parameter

$$\xi = \frac{Z_1 Z_2 A_1^{1/2} E_r'}{12.65 (E_1 - \frac{1}{2} E_r')^{3/2}} [1 + \frac{5}{32} (\frac{E_r'}{E_1})^2 + \dots]$$

with the abbreviation $E_r' = (1 + A_1/A_2) E_r$. The values for $f_{E1}(\eta, \xi)$ are given in Ref. /15/ in the classical approximation $\eta \to \infty$. For all practical purposes, the approximation can be used if $n \geq 100$. In all of our investigations with Ni, Ge, Kr, Nb, La and Bi ions this relation was fulfilled. The factor $(Z_1/A_1 - Z_2/A_2)^2$ in formula (5) indicates that in a closed system of particles characterized by $Z_i/A_i = \text{const}$, no electrical dipole radiation can arise. Higher multipolarities will be important but with much slower intensity and the energy loss of the incident ions is caused only by recoil effects and ionization processes.

The contributions, calculated in this way, of both electronic and nuclear bremsstrahlung (SEB and NNB) to the X-ray continua measured in the collisions Zr + Nb, Nb + Nb and Mo + Nb (96 MeV Nb ions) are illustrated in Figure 4. The triangles and circles represent the spectra of the nuclear and electronic bremsstrahlung, respectively, whereas the dashed-dotted line represents the mean backgrouns measured in a delayed regime. Finally the dashed line gives the summed spectrum of bremsstrahlung and delayed background. Figure 4 demonstrates that the X-ray continua at energies above the energy of the characteristic atomic KX-radiation cannot be explained as due to these bremsstrahlung processes. For example, the yield integral computed for the X-ray energy range between 16 keV and 30 keV is at least three orders

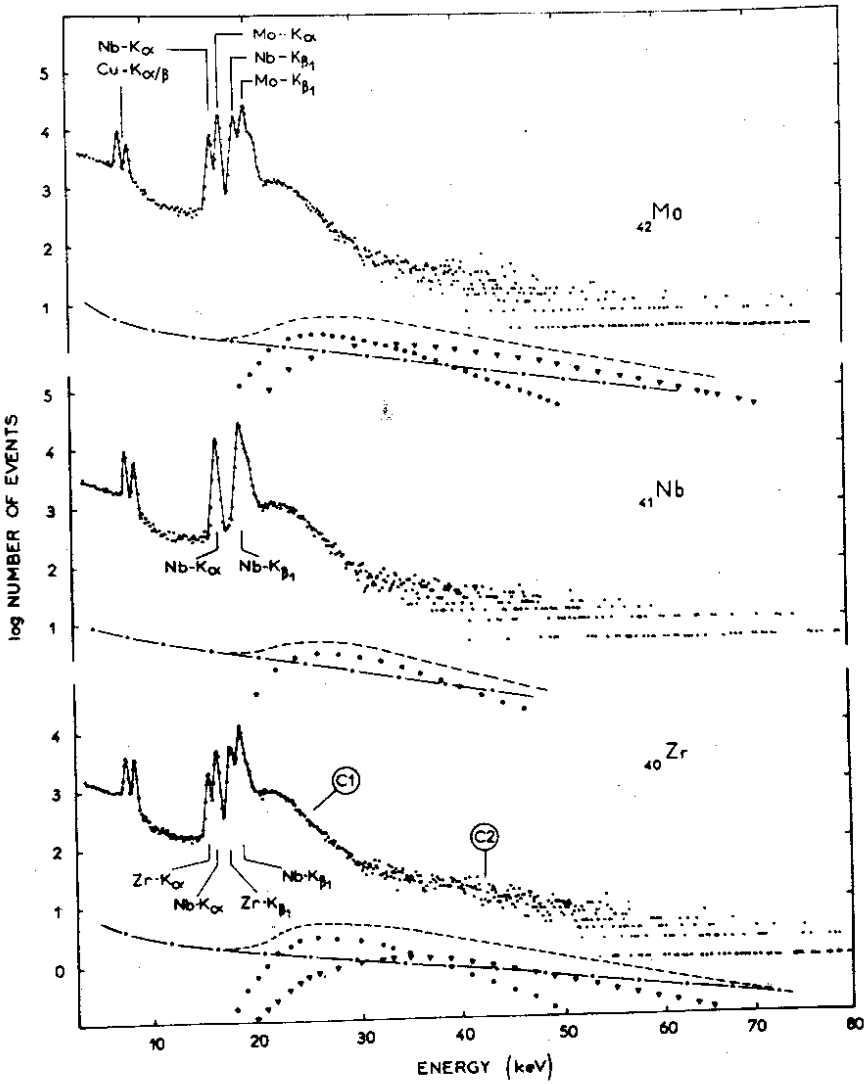

Fig. 4. The contributions of bremsstrahlung to the X-ray continua obtained in the collisions Zr + Nb, Nb + Nb, and Mo + Nb (96 MeV Nb ions, Ref. /12/).

of magnitude smaller than the values measured. Also the slope is wrong. After correcting for the detector efficiency and absorber attenuation the linear extrapolation of the spectra in a logarithmic representation shows that the experimental yield goes down like E_r^{-n} with $n \approx 20$. This disagrees drastically with the value $n \lesssim 7$ obtained in our calculations. Radiative electron capture (REC) into the projectile K-shell forms a peaked spectrum centered around $E_X = E_K + \frac{1}{2} m_e v_1^2$, where E_K is the projectile k ionisation energy. For a typical projectile velocity of 10^9 cm/sec., the energy $\frac{1}{2} m_e v_1^2$ is lower than 1 keV. For this reason the REC effect is observable clearly only for collision systems with lower Z and at higher incident energies. For example, Figure 5 shows this effect measured in Al + 90 MeV S collisions /16/. Hence, the important question arises as to how intense the high-energy tails of these REC spectra are in collisions of heavy atoms. The present-day calculations on this point are not yet firm. To examine the possible effect of the REC-tails in our experiments, we investigated X-ray spectra by bombarding gas targets. Figure 6 shows the experimental set-up and the X-ray spectrum measured for the collision system Kr + Kr (42 MeV).

A ^{84}Kr ion beam reaches, through a thin Ni foil, a target filled with gaseous Kr at a pressure of 60 torr. The experimental geometry is such that the Ge detector is capable of detecting only those X-rays which are produced in the gas volume located rather far from the Ni foil. Thus, the K-vacancies produced in the projectile as they

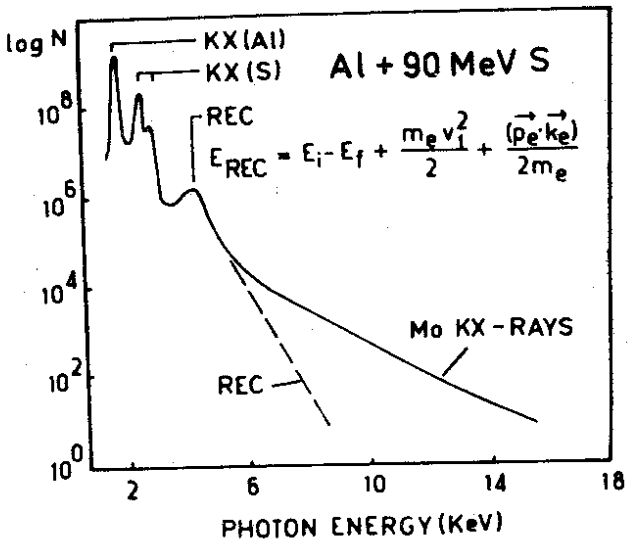

Fig. 5. The REC effect measured in Al + 90 MeV S collisions (Ref. /16/).

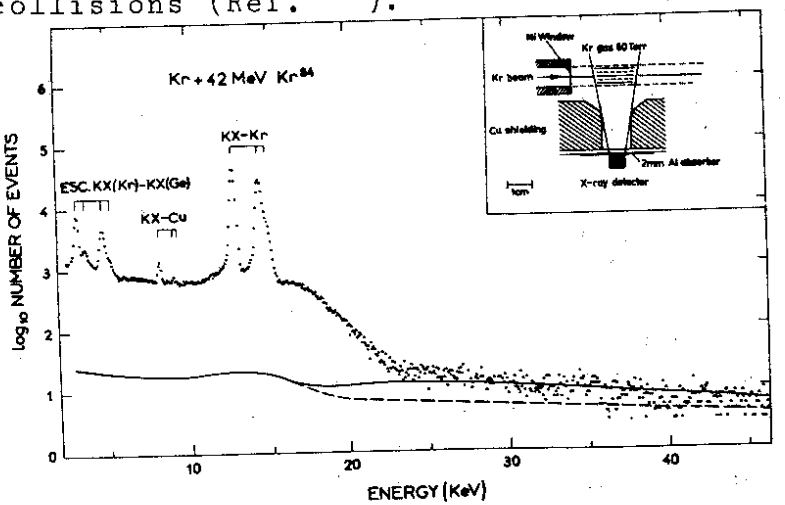

Fig. 6. The X-ray spectrum measured by bombarding the Kr gas target with 42 MeV Kr ions.

pass through the foil are already filled and cannot cause the REC effect in the spectra measured. The X-ray spectrum exhibits the characteristic atomic KX-lines of krypton and Cu absorber and, in addition, a continuum whose properties are similar to those of the continuous X-ray spectra of solid targets. The obvious presence of this intensive continuous component in experiments with a gas target provides evidence for the fact that this component cannot be caused by radiative electron capture.

On the other hand, all the background continua discussed here are small compared to the experimental continua in our experiments. For this reason these continua were assumed to be the molecular orbital radiation due to radiative decay of vacancies in transiently formed quasi-molecules.

3. Two Components of the Quasi-Molecular KX -Ray Spectra

We first showed in our experiments with Ge,, Nb and La ions [6,8,9] that the quasi-molecular KX-ray continua consist of a low-energy and high-energy component, denoted by us as (C1) and (C2), respectively. In Figure 7 are plotted the absolute X-ray intensities corrected for absorption and detector efficiency taken in Nb+Nb collisions (67 MeV). The full line indicates the summed spectrum of the mean background measured and the calculated electronic bremsstrahlung [12]. This figure shows also that the continuum (C1) is a real physical

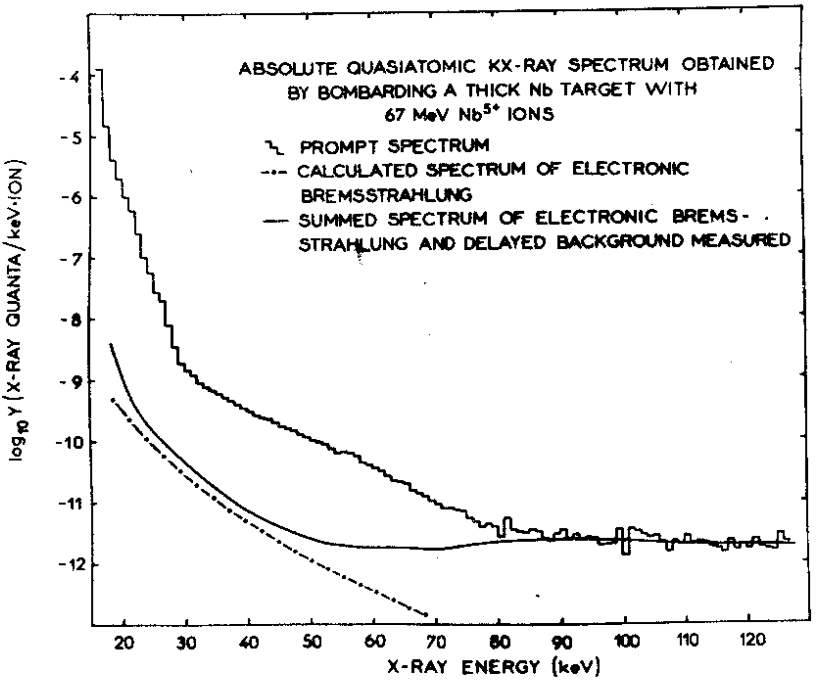

Fig. 7. The quasi-molecular X-ray spectrum of the Nb+Nb (67 MeV) system corrected for absorption and detector efficiency.

effect and the continuous X-ray spectrum has the two-component structure. The high-ehergy part (C2) of the continuum has been identified as quasi-molecular KX-radiation. Besides the properties of the component (C2), the physical nature of the low-energy continuum (C1) is of special interest. Electronic and nuclear bremsstrahlung and also the REC process cannot account for the continuum (C1). Recently, Heinig et al. /17/ tried to give an explanation for the origin of the component (C1), which may take place

during the transient formation of quasi-molecules. The authors pointed out that in all molecular correlation diagrams for medium atomic numbers Z_1 and Z_2 reported till now, the $2p\sigma$ term shows a relative minimum. This is shown in Figure 8 with the correlation diagram for quasi-molecular states of the system $_{41}Nb+_{41}Nb$ as an example. The energies of the quasi-molecular states are calculated here by N.Truskova [18] by solving a non-relativistic problem with a two-cetnre potential and a fixed internuclear distance. The $2p\sigma$ term joins the L- or K-shells of the colliding particles in the limits of the united or separated atoms, respectively. Therefore, in the electron promotion model the L-vacancies must be transferred in a collision via this term to the K-shells of the separated atoms. Figure 9 shows schematically this simplest electron promotion process for symmetric collisions. A linear representation of other correlation schemes published demonstrates that allowed transitions from higher terms to the "$2p\sigma$ minimum" have a higher energy than the transitions owing to the characteristic lines. Figure 10 shows this fact for symmetric collision systems. In addition, one can see that the maximum binding energies $E_{max}(2p\sigma, 2Z)$ of quasi-molecular $2p\sigma$-levels agree with the endpoint energies of the Cl components measured in our experiments with Ge, Kr, Nb and La ions. For that reason it is suggested by Heinig et al. [17] that tha continuum (Cl) is produced by such transitions. According to these suggestions the high intensity of the continuum (Cl) can be explained assuming that the vacancies

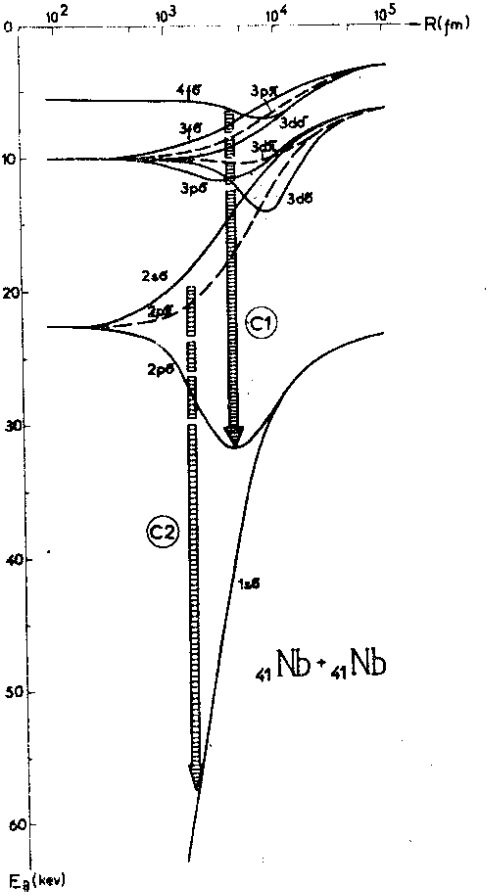

Fig.8. The molecular level diagram of the Nb+Nb collision system.

in the 2pσ minimum were filled mostly in a first collision, whereas a second collision is assumed to produce the continuum (C2). Following Meyerhof et al.[19], a crude order-of-magnitude estimate of the expected yield ratios Y_{C1}/Y_{C2} for symmetric collisions can be given. We assume that the 1sσ vacancy production by a two-step process dominates. Let Y_p be the 2pσ vacancy yield per projectile in a "primary" collision (see Figure 9). After the decay of the quasi-molecule such a 2pσ vacancy manifests itself as the K vacancy in the projectile with a probability of nearly 50%. If the mean life time τ_K of this K vacancy is sufficiently long it will give rise to the formation of a 1sσ vacancy in a secondary collision again with a 50% probability. Then the total C2 yields is

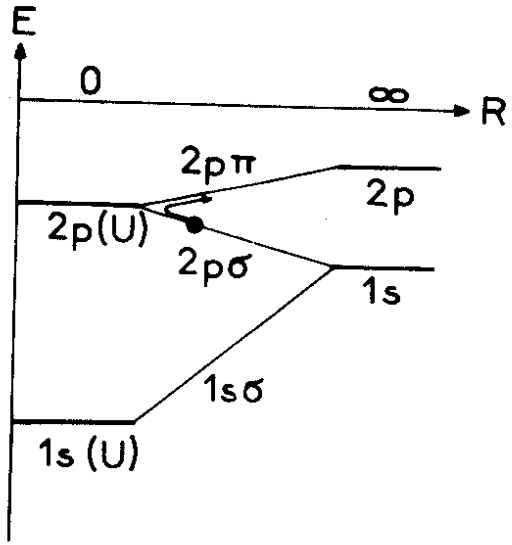

Fig.9. Schematic molecular level diagram for a symmetric collision. Only levels relevant to K-vacancy formation are shown.

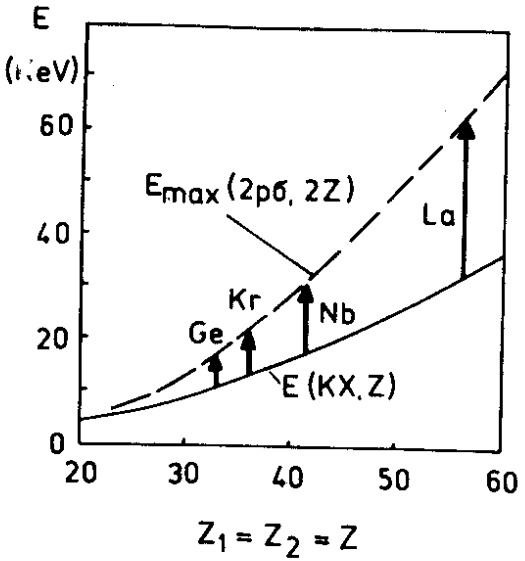

Fig.10. The maximum binding energies of quasimolecular $2p\sigma$ states as a function of atomic number and the "endpoint" energies of the Cl components measured in our experiments.

$$Y_{C2} = \frac{1}{4} Y_p \left(\frac{v_1 \tau_K}{d}\right) P_K \frac{t_{C2}}{\tau_{1s\sigma}} . \qquad (6)$$

Here, v_1 is the velocity of the projectile, d is the distance between the atomic planes, and P_K is the probability of the overlap of projectile and target K orbits in one atomic plane. The quasi-molecular formation time t_{C2} is expressed by a cut-off radius r_{C2} between colliding nuclei $t_{C2}=2r_{C2}/v_1$. Quasi-molecular X-ray radiation which contributes to the continuum (C2) can be emitted only in close collisions with an impact parameter $b < r_{C2}$. The total C1 yield can be estimated using the expression

$$Y_{C1} = Y_p \left[\frac{1}{2} \cdot \frac{t_{C1}}{\tau_{2p\sigma}} + \frac{1}{4} \left(\frac{v_1 \tau_K}{d}\right) P_{LK} \frac{t_{C1}}{\tau_{2p\sigma}}\right], \qquad (7)$$

where $t_{C1} = 2r_{C1}/v_1$. The first term of this formula describes the quasi-molecular radiation emitted after the $1p\sigma$ vacancy production in the primary collision. It is reasonable to assume $r_{C1} \geq 10 r_{C2}$ and, consequently, also $P_{LK} > 100 P_K$, $\tau_{1s\sigma} \approx \tau_K / 10$, $\tau_{2p\sigma} \approx \tau_K$. Under these assumptions this simple model gives, for the collision systems investigated by us, the ratios $Y_{C1}/Y_{C2} \geq 10^2 - 10^3$, which agree with our experimental results.

In order to obtain additional experimental information about the proposed quasi-molecular origin of both components (C1) and (C2) of the X-ray continuum, we have performed an experiment aimed at the determination

of the velocity of the radiative system using the X-ray energy Doppler shift in the collisions Nb + Nb(67 MeV). A similar experiment has recently been carried out by Meyerhof et al.[20] for the high-energy part of the continuum in the collisions Zr + Kr (200 MeV). The essence of this experiment is as follows (see Figure 11). As a function of the velocity of the radiative system, the energies of the X-rays emitted obtain a Doppler shift which can be determined by detecting X-rays at different angles with respect to the ion beam direction. The Doppler velocity characterizes the radiative system irrespective of the details of the assumed production mechanism for the X-ray continuum. In particular, if radiation in a certain X-ray energy region is believed to originate from quasi-molecular processes, the Doppler velocity should be equal to the cetnre-of-mass velocity $V_{c.m.}$, of the intermediate molecules. Figure 11 shows the principal experimental arrangement used to measure the Doppler velocity. The metallic Nb target, 1 mg/cm^2 thick, was placed at $\pm 45^\circ$ with respect to the ion beam. The measurements were made at the laboratory angles $\theta = -90^\circ$, 45°, 90° and 135°. Each spectrum was normalized to the intensity of the Nb+K_α line which had an isotropic angular distribution. Figure 12 shows the results of these measurements. In figs. 12a and 12b we present the ratios of the normalized spectra at $+90^\circ$ and -90° and at 45° and 135°, respectively, as a function of the X-ray energy in the laboratory system. The asymmetry seen in fig. 12b occurs as a result of the fact that at angles of 45°

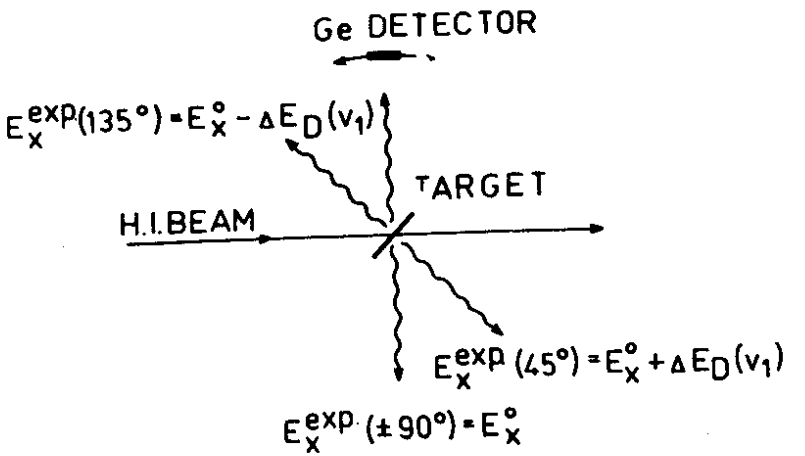

Fig. 11. The principal experimental arrangement for Doppler shift measurements.

and 135° the X-ray energy Doppler shift has an opposite sign. The ratios of the spectra at 45° and 135° taking into account the Doppler shift in the cases of the velocity $V_{c.m.}$ of the intermediate molecules Nb+Nb and V_∞ of the 67 MeV Nb projectiles are shown in figs. 12c and 12d, respectively. Figure 12c shows that in the energy regions of both continua, (C1) and (C2), X-rays are emitted from systems having velocity $V_{c.m.}$ of the quasi-molecule Nb+Nb. From this fact we conclude that both components of the X-ray continuum, (C1) and (C2), originate from quasi-molecular transitions. Thus, their previous interpretation is confirmed by this independent experiment with Doppler shift measurements.

It is important to determine the Doppler shift of the continuum X-rays from heavy-ion collisions also for another reason. In the

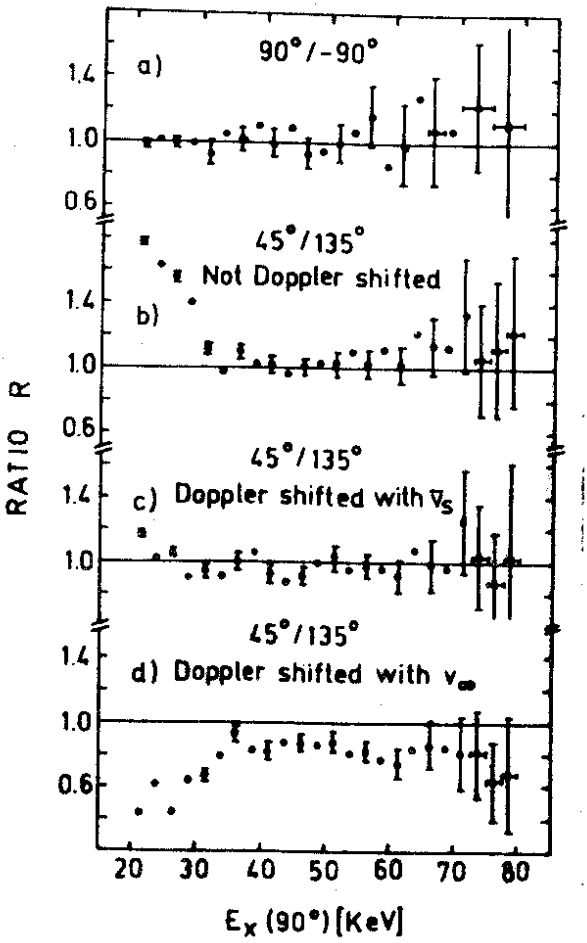

Fig. 12. Ratios of normalized X-ray spectra from Nb+Nb collisions (67 MeV Nb ion), without (a) (b) and with (c) (d) the Doppler shift correction made.

interpretation of the laboratory anisotropy of the continuum X-ray spectrum, knowledge of the Doppler velocity is needed in order to compare the measured anisotropy with the theoretically predicted c.m. anisotropy of the quasi-molecular X-rays. It has been shown that dynamic effects play an important role in the shape of the X-ray continua observed in heavy ion-atomic collisions [21] . They cause a smearing of the quasi-molecular X-ray distributions beyond the K energy limit of the united atom and lead to induced transitions between molecular electronic states. These induced transitions originating as a result of the rotation of the internuclear axis add incoherently to the so-called spontaneous molecular transitions. The sum of these two parts of quasi-molecular X-radiation produces the anisotropy of the spectra with respect to the incident beam direction. The rapid variation of the anisotropy near the united atom energy limit indicates a quasi-molecular phenomenon, but further experimental and theoretical developments are needed to clarify the origin of the anisotropy. Our Dubna group started investigations with the anisotropy of quasi-molecular KX-rays for the system Ni + Ni (67 MeV) and obtained the same results as those of Greenberg et al. [22]. Figure 13 shows that in Ni + Ni collisions the asymmetry $\eta(E_x)$ of the quasi-molecular KX-radiation shows a maximum at an X-ray energy of $E_x \simeq 32$ keV, where the KX-radiation of the united atom ($Z = 56$) is expected. The values of η without and with the Doppler correction are of the same order of magnitude as those obtained by Greenberg et al. [22].

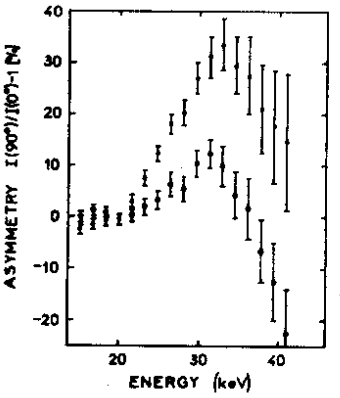

Fig. 13. The asymmetry $\eta = I(90°)/I(0°) - 1$ of the quasi-molecular KX-radiation obtained in the Ni +67 MeV Ni measurement.

Recently, we have carried out measurements of X-ray asymmetry in the region of quasi-molecular continua (C1) and (C2) in the systems Nb + Nb (67 MeV) and Ge + Ge (54 MeV). After determining the Doppler velocity for these cases in the experiment described above one could correct the observed spectra for this effect and determine reliably the behaviour of the anisotropy as a function of the X-ray energy. The results of Nb + Nb experiments are shown in Figure 14. Open and closed circles denote the η values without and with Doppler correction, respectively. This correction was introduced by the formula $E_{i,m} = E_i(1 + \bar{v}_s/c \cos\theta)$, where $E_{i,m}$ is the energy measured within an energy interval $\{i\}$, $v_s = 1/2\pi/4v_\infty$ is the mean c.m. velocity in the system Nb + Nb (67 MeV) and θ is the photon emission angle. The v_s value has been calculated by integrating over all impact parameters corresponding to classical ion trajectories which cross the K-shell radius of the Nb atom. One can see that the asymmetry has two maxima in the energy regions of 29 keV and 80 keV, which just correspond to the maximum energies of the two continuum compo-

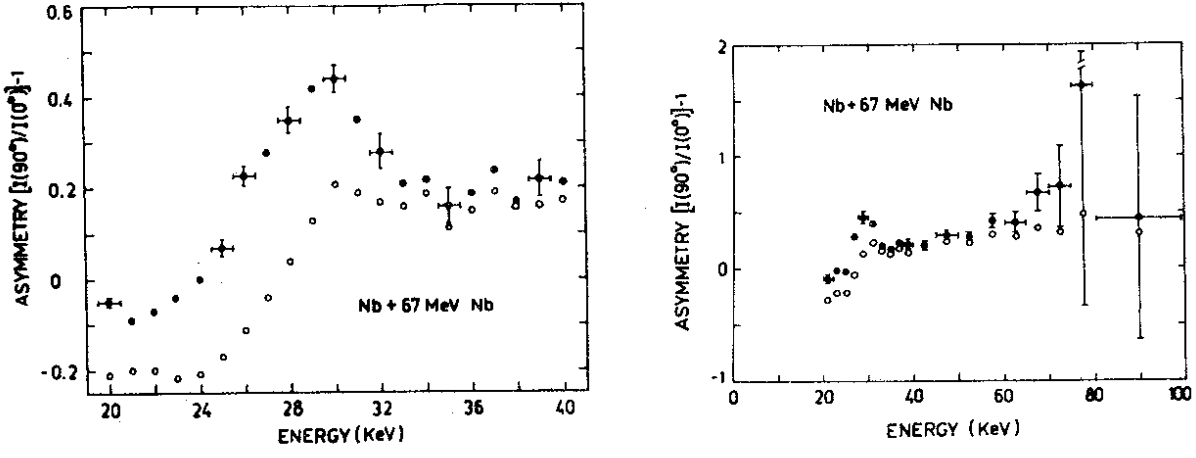

Fig. 14. The asymmetry η of the quasi-molecular X-ray spectra obtained in the Nb + 67 MeV Nb measurement. The open and closed circles show the η values without and with the Doppler correction, respectively.

nents (C1) and (C2) of the quasi-molecular spectrum observed by us. At the same time they correspond to the maximum energies of possible transitions of the quasi-molecule Nb+Nb to the $2p\sigma$ and $1s\sigma$ states at small internuclear distances (see Figure 8). This indicates that these new results on the angular asymmetry of quasi-molecular continua (C1) and (C2) provide at least additional independent experimental evidence in favour of the previous interpretation of quasi-molecular KX-ray spectra as having the two-component structure.

These results and conclusions were substantiated by the investigations of other collision systems, made recently by our group at Dubna. Figure 15 shows the X-ray spectrum obtained by bombarding a ^{74}Ge target with 54 MeV ^{74}Ge ions. The continuous quasi-molecular spectrum clearly consists of two parts differing in energy and intensity. This is in full analogy to the observation of the components (C1) and (C2) in the case of Nb+Nb collisions. One can see in Figure 16 that the asymmetry of quasi-molecular X-rays has also two maxima at X-ray energies, which correspond to the maximum energies of the quasi-molecular components (C1) and (C2).

Finally, we sum up the main qualitative conclusions drawn from our experiments. They are:

(i) In all symmetric collision systems with $Z_1=Z_2=Z \geq 32$ the X-ray continua observed at energies higher than the energy of the characteristic KX-radiation of separate atoms have a well-pronounced two-component structure.

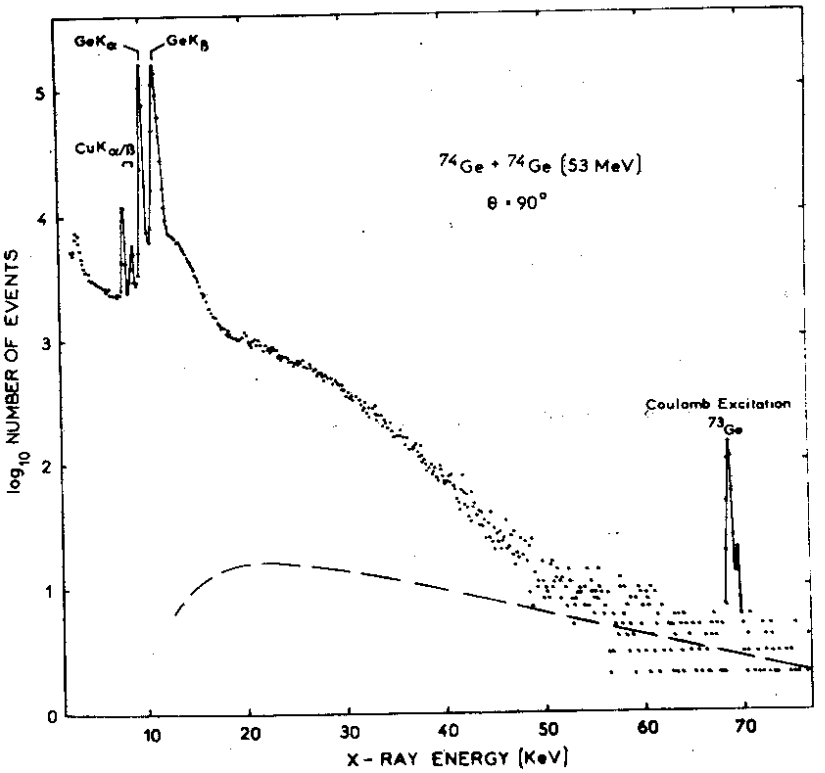

Fig. 15. The X-ray spectrum measured by bombarding the ^{74}Ge target with 53 MeV ^{74}Ge ions.

(ii) The experiments on the determination of the Doppler velocity of the radiative system, the measurements of the angular asymmetry of these spectra, as well as the experiments using a gas target indicate the quasi-molecular origin of both components.

(iii) The features of these components established by us agree qualitatively with the assumption that the continuum (C1) is

associated with quasi-molecular transitions to the $2p\sigma$ states, and the continuum (C2) with transitions to the $1s\sigma$ states of quasi-molecules with a double atomic number.

A sime-quantitative verification of this picture by a dynamical theory of intermediate molecular phenomena is given recently by the Rossendorf group and our group in ref. /23/.

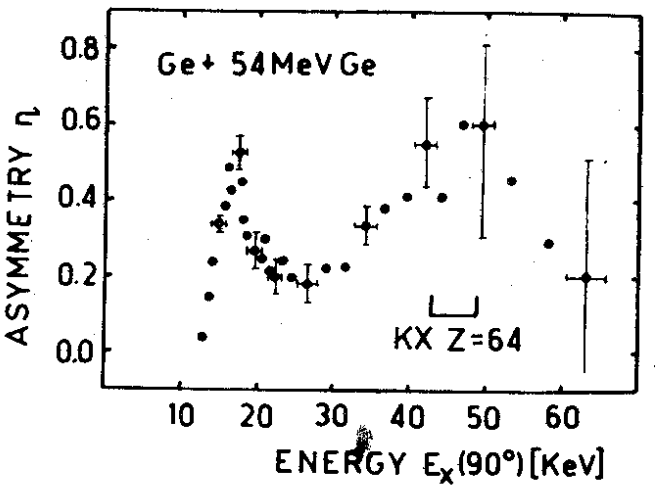

Fig. 16. The asymmetry η of the quasi-molecular X-ray spectra obtained in the Ge + 53 MeV Ge measurement.

4. The Spectral Distribution of Quasi-Molecular X-Rays and Comparison with Experimental Results

To describe the gross structure of high-energy quasi-molecular X-ray spectra emitted in symmetric ion-atom collisions, we apply the dynamical theory of intermediate molecular phenomena in heavy ion scattering. A similar approach has been employed by Macek and Briggs /24/ in their study of quasi-molecular KX-ray transition in high collision systems. Contrary to the treatment of Mecek and Briggs, we take also into account the possible radiative decay of $2p\sigma$ vacancies immediately after their formation by $2p\sigma-2p\pi$ promotion in "primary" collisions, the interference term between the atomic lines and the $2p\sigma$ radiation from such primary collisions, and the quasi-molecular $1s\sigma$ and $2p\sigma$ radiation emitted during secondary collisions between target atoms and a projectile having already a K-vacancy.

A general description of the radiation processes in heavy ion collisions have been given recently by Smith et al. /25/. Expanding the total wave function of the collision problem on stationary atomic or molecular states plus one-photon states and assuming adiabatic motion, they calculated the spectral amplitude of the emitted photons in first order of perturbation theory. If the rotationally induced radiative decay of innershell vacancies is neglected, one obtains (in dipole approximation) the formulae for the spectral yield per vacancy

$$I_i(\omega) = \frac{4e^2\omega}{3c^3\hbar} \sum_f |\vec{D}^c_{fi}(\omega)|^2 . \qquad (7)$$

$$\vec{D}^c_{fi}(\omega) = (2\pi)^{-1/2} \int_0^\infty \vec{D}_{fi}(R(t)) \exp[i\omega t - i\int_0^t \bar{\omega}_{fi}(R(t'))dt' - \frac{\Gamma}{2}t]dt , \qquad (8)$$

which has been already extensively discussed and applied to $2p\pi-1s\sigma$ electronic transitions by Macek and Briggs /24/ . We start from the same formulae, but evaluate them in the framework of our special assumptions on the collision process. First, we consider the collision of a projectile having L vacancies. It is assumed that at the distance of closest approach (at time $t_1 = 0$) with a certain probability one of these L vacancies is transferred to the $2p\sigma$ orbital by $2p\sigma-2p\pi$ electron promotion. After this "primary" collision the $2p\sigma$ vacancy appears with the probability 1/2 as K vacancy in the projectile which is moving through the solid, and can form quasi-molecules with target atoms in secondary collisions (at times $t=t_j-T_c/2,...,t_j+T_c/2$; $j = 2,3,...,$; T_c is the collision time). In such a way, our initial state $|i\rangle$ having an innershell vacancy with total decay rate Γ is time dependent for every close collision. This time dependence enters the description through the mutual internuclear distance, $R = R(t)$, between the ion and its collision partner. The decay of the vacancy state by radiative decay to different final states $|f\rangle$ is described by the transition energy

$$h\bar{\omega}_{fi}(R) = E_i(R) - E_f(R) \qquad (9)$$

and the dipole matrix element

$$\vec{D}_{fi}(t) = \langle f|\vec{v}|i\rangle = -i\bar{\omega}_{fi}(t)\langle f|\vec{r}|i\rangle \qquad (10)$$

which can be expressed by velocity $\vec{v}$ or coordinate $\vec{r}$ of the jumping electron. Further approximations (semi-quantitative non-relativistic correlation diagrams, constant dipole matrix elements, no vacancy transfer to target atoms), and details of the calculations are described in ref. /23/. Here I would like to give only the comparison of calculated photon yields with experimental results. In Figure 17 this comparison is made with the data obtained from the Ni + + 39 MeV Ni experiment. In this measurement a thin target (85 $\mu g\ cm^{-2}$)of natural Ni has been used. The spectrum obtained was corrected for detector efficiency. The delayed room background, electronic and nuclear bremsstrahlung /12/ have been subtracted. Figure 17 shows the theoretical yield per vacancy $I(\omega)$ and also the contributions of strong radiative transitions to this quantity calculated by us /23/. Since we take into consideration the interference between central atomic lines and the quasi-molecular $2p\sigma$ transitions from primary collisions, only the sum of quasi-molecular $2p\sigma$ radiation and central line wigns can be presented. At photon energies $E_x = 10 \div 25$ keV, we obtain an absolute spectral distribution $I(\omega)$, which is very similar to the measured one. We think that the achieved agreement

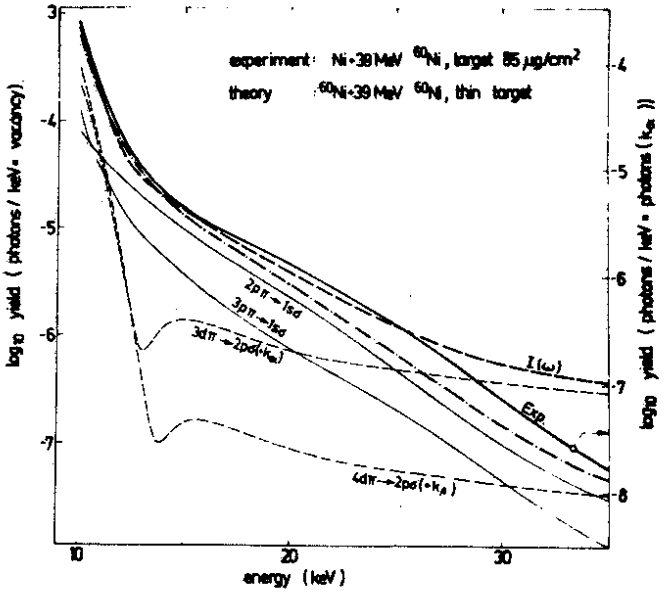

Fig. 17. Comparison of experimental (solid line) and theoretical (dashed line) photon yields in Ni + 39 MeV Ni collisions.

strongly supports both the suggestions on the appearance of two quasi-molecular components in the spectrum and the assumptions on the reaction mechanism adopted in this calculation.

In Figure 17, the contributions from quasi-molecular transitions to the $2p\sigma$ state range, in practice, only up to about E_x = = 15 keV. Above this energy, the two corresponding curves consist of pure K_α and K_β line tails, respectively. Especially, above $E_x \approx 25$ keV the deviations of $I(\omega)$ from experiment which arise in the same energy region seem to be closely related to this

dominance of the K_α line tail. If the atom line contribution is omitted formally in the calculation of the spectrum (dashed-dotted line in Figures 17 and 18), one obtains, at high frequencies, an essentially better agreement with experiment. This result suggests to think about line profiles at frequencies far from the line center (here $\omega \geq 4\omega_0$, , $\Gamma \ll \omega_0$). In the general consideration leading to a Breit-Wigner distribution $I(\omega) \sim \omega / [(\omega - \omega_0)^2 + \Gamma^2/4]$ it is provided in the framework of a two-state approximation that the decay of the excited state at time $t = 0$ suddenly begins. The validity of these initial conditions in our cases requires a more careful investigation. Using the uncertainty relation $\Delta E \cdot \Delta t \approx \hbar$ one can see that the emission of photons with energies $h_\omega = h_{\omega_0} + \Delta E$ far ($\Delta E \approx 20$ keV) from the transition energy $\hbar\omega_0$ depends on perturbed initial conditions during a short time interval of the order $\Delta t \approx \hbar/\Delta E \approx 10^{-19}$ s. These are just times which characterize the vacanvy production by electron promotion. Thus, the deviations from experiment at high photon energies should be due to the separate treatment of vacancy production and vacancy decay. This effect is discussed in more detail recently by Heinig et al. [26]. A qualitative comparison of thick-target measurements and theoretical spectral yields is given in Figure 18. Such a comparison is still meaningful since the radiation yield per vacancy $I(\omega)$ weakly depends on the impact energy. Nevertheless, the comparison made in Figure 18 for the collision systems Ni + 67 MeV Ni , Ge + 81 MeV Ge and Nb + 67 MeV Nb reveals completely the same kind of agreement between theory

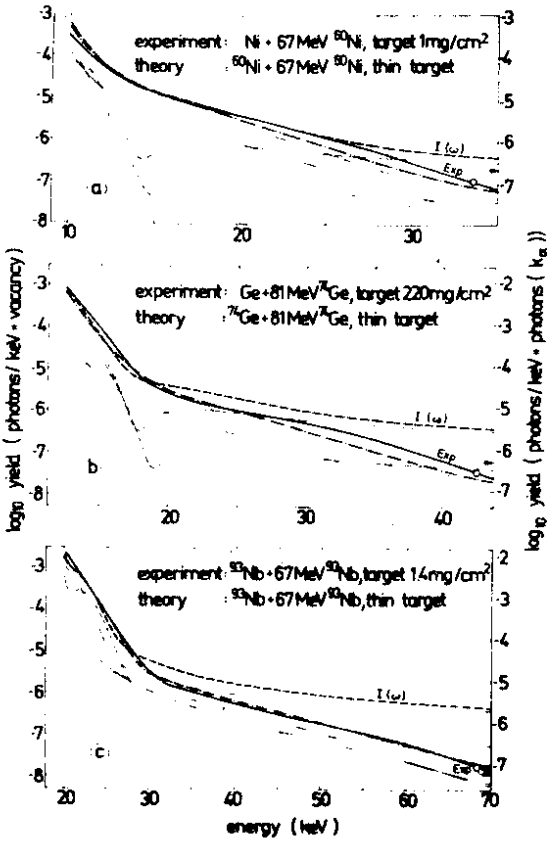

Fig. 18. Qualitative comparison of thick-target measurements and theoretical spectral yields per vacancy for Ni + Ni, Ge + Ge, and Nb + Nb collisions.

and experiment as has been discussed above already for the Ni + 39 MeV Ni system. Here I will not discuss the question of oscillations in quasi-molecular spectra which can be caused by the interference effects of radiative processes in heavy ion collisions.

We have not obtained such oscillations in our experimental investigations.

5. Summary

A relatively consistent picture of the two-component structure of high-energy quasi-molecular X-ray spectra has emerged from symmetric collisions with very heavy ions. The calculations in the framework of the dynamical theory reproduce the two-component structure of high-energy X-ray continua. In all cases of symmetric collision systems we have obtained the rapid c variation of the anisotropy of quasi-molecular radiation at the maximum binding energies of the quasi-molecular $1s\sigma$ and $2p\sigma$ states, but further experimental and theoretical investigations are needed to clarify the origin of the anisotropy. It is possible that the anisotropy effect can be used to perform spectroscopy of arbitrary two-center levels, and especially the spectroscopy of superheavy quasi-atoms as a most important problem (QED in overcritical fields!). The future experiments on the investigation of the asymmetry of quasi-molecular radiation for very heavy systems ($Z \gg 100$) will require ion beams with intensities higher than 10^{12} ions/sec. In our first experiments with Bi ions we have shown that the cross section for the production of K-vacancies is very low (see Figures 19 and 20). They turned out to be equal to $\sigma(KX - Bi, 144 MeV) = 1.6 \times 10^{-26}$ cm^2 and $\sigma(KX - Bi, 172 MeV) = 1.2 \times 10^{-25}$ cm^2. The order of magnitude

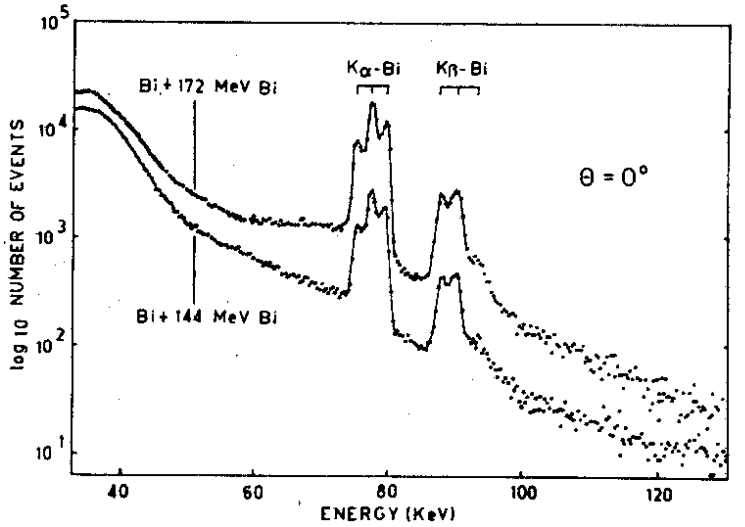

Fig.19.The X-ray spectrum measured by bombarding the Bi target (1 mg/cm^2) with Bi ions.

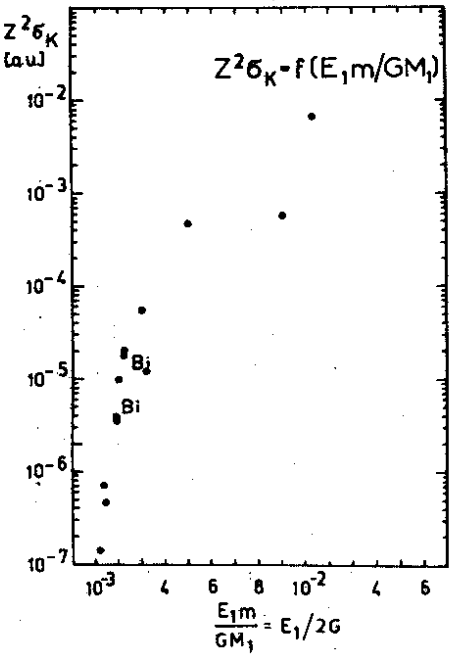

Fig.20.The experimental K-vacancy production cross section scaled according to the scaling law,given by Meyerhof et al. /27/.

of these values agrees with the scaling law for higher - Z collisions, given by Meyerhof et al. /27/. Irrespective of these "pessimistic values" of the positron production cross section in U+U collisions, the observation of X-ray radiation of superheavy quasi-atoms promises to be an interesting field of investigation for the nex few years. The search for positron emission from processes in overcritical fields of superheavy quasi-atoms must await the availability of suitable heavy-ion accelerators.

References

1. M.Barat, W.Lichten. Phys.Rev., A6, 211 (1972).
2. B.Muller et al. Phys.Lett., 53B, 401 (1975).
3. J.Rafelski et al. Phys.Rev.Lett., 27, 958 (1971).
4. V.S.Popov. Sov.Phys., JETP, 32, 256 (1971).
5. W.Frank et al. JINR, E7-9427, Dubna, 1975; Z.Physik, A277, 333 (1976).
6. P.Gippner et al. Nucl.Phys., A230, 509 (1974).
7. K.-H.Kaun et al. JINR, E7-9629, Dubna, 1976;
8. P.Gippner et al. Phys.Lett., 52B, 183 (1974); W.Frank et al. Z.Physik, A277, 333 (1976); JINR, E7-9861, Dubna, 1976.
9. W.Frank et al. Phys.Lett., 58B, 41 (1975); JINR, E7-9029, Dubna, 1975.

10. K.-H.Kaun et al. JINR, E7-9629, Dubna, 1976;
11. P.Arnbruster et al. Physica Scripta, 10A, 175 (1974).
12. P.Gippner. JINR, E7-8843, Dubna, 1975.
13. F.Folkmann et al. Nucl.Instr.Meth., 116, 487 (1974).
14. J.D.Garcia. Phys.Rev., 117, 223 (1969); Phys.Rev., A1, 280 (1970).
15. K.Alder et al. Rev.Mod.Phys., 28, 432 (1956).
16. H.-D.Betz et al. Phys.Rev.Lett., 34, 1256 (1975).
17. K.-H.Heinig et al. Phys.Lett., 60B, 249 (1976).
18. N.F.Truskova. JINR Report,P11-10207,Dubna, 1976.
19. W.E.Meyerhof et al. Phys.Rev.Lett., 32, 1279 (1974).
20. W.E.Meyerhof et al. Phys.Rev., A12, 2641 (1975).
21. B.Muller et al. Phys.Lett., 49B, 219 (1974); Phys.Rev. Lett., 33, 469 (1974).
22. J.S.Greenberg et al. Phys.Rev.Lett., 33, 473 (1974).
23. K.-H.Heinig et al. JINR, E7-9862, Dubna, 1976; submitted to the J.Phys.B.
24. J.-H-Macek, J.S.Briggs. J.Phys., B7, 1312 (1974).
25. K.Smith et al. J.Phys., B8, 75 (1975).
26. K.-H.Heinig et al. Preprint ZfK Rossendorf, submitted to the Phys.Letters.
27. W.E.Meyerhof et al. Phys.Rev., A11, 1083 (1975).

Received by Publishing Department
on December 30, 1976.